Size-effects in the chemical modification of carbon black nanoparticles with 4-nitroaniline

Janjira Panchompoo, Leigh Aldous and Richard G. Compton*

Received (in Montpellier, France) 27th May 2010, Accepted 8th July 2010
DOI: 10.1039/c0nj00400f

The chemical modification of a range of carbon blacks (primary particle diameters ranging from 14 nm to 66 nm) has been investigated and characterised by means of cyclic voltammetry (CV), X-ray diffraction (XRD), X-ray photoelectron spectroscopy (XPS) and acid–base Boehm titration. An electrochemical probe molecule, 4-nitroaniline, was introduced to the carbon black. Physisorption and intercalation processes were observed and quantified electrochemically. Significantly more 4-nitroaniline per cm^2 was present for smaller particles, implying extensive intercalation for particles *ca.* 14 nm in diameter. The voltammetric reduction of 4-nitroaniline covalently tethered to the carbon black was observed at a potential *ca.* 0.4 V more negative than the physisorbed and intercalated species, allowing separate quantitative analysis. Nanoscale size effects of carbon black were observed, with an optimum size of 27 nm observed. The electrochemical responses regarding the physisorption process decreased with the increase in surface oxidative pre-treatment time. In contrast, voltammetric signals corresponding to covalently tethered 4-nitroaniline increased with surface oxidation, before decreasing due to over-oxidation of the carbon black. The importance of some oxidation in forming electrochemically stable covalently-tethered groups is noted and discussed.

1. Introduction

Carbon materials are widely employed as electrodes, and surface species are well known to influence electrochemical processes carried out at such electrodes. The identification, quantification, introduction, *etc.* of oxygen-containing species has long been a topic of interest.[1–5] For example, the use of carbon electrodes in fuel cells can result in oxidation of their surfaces, detrimentally altering their material properties.[6,7] The direct electrochemical investigation of the carbon material[8,9] and employment of electrochemical probe molecules to fingerprint and quantify specific groups[5–7,10] are attractive, sensitive approaches that require only micrograms of sample.

The deliberate modification of carbon surfaces is also of interest, due to the introduction of functionality. Possible reasons include the introduction of electrochemical functionality,[11,12] to enhance metal sorption,[13–15] to support the formation and growth of nanoparticles on surfaces,[16,17] and for energy-storage devices, *e.g.* supercapacitors.[3,18]

Carbon black consists of carbon particles generated by the incomplete combustion of a hydrocarbon. They consist of 'primary' particles, which are frequently spherical in shape, and are invariably fused into larger aggregates.[19] The aggregates have a significant effect upon bulk properties, although the quasi-graphitic microstructure associated with the primary particle size will influence surface properties. A huge number of carbon black varieties are commercially available in bulk, with a multitude of physical and material properties. Primary electrochemical interest into carbon black materials stems from their application in fuel cell devices.[3,4,6,7]

The modification of carbon materials for electrochemical and other applications has frequently employed well-defined materials such as glassy carbon[6,12–14] and carbon nanotubes.[5,10,17,20–24] However, such materials are still relatively expensive. Graphite[15,22–24] is a significantly cheaper alternative, although a poor surface-to-mass ratio inevitably means large amounts of graphite are required to match the functionality of much smaller quantities of carbon nanotubes. Carbon black, being a cheap, widespread material consisting of relatively small particles with a quasi-graphitic microstructure, is a possible alternative.

This work has investigated the modification of carbon black with 4-nitroaniline, as an electrochemical probe molecule. A number of studies were carried out in order to investigate the modification of carbon black, with electrochemical and physical characterisation of the resulting materials. The surface interaction (physisorption and intercalation) of 4-nitroaniline on carbon black was investigated. The covalent tethering of 4-nitroaniline to carboxylic acid (and other) surface groups was also investigated. Both of these studies were conducted as a function of (a) primary particle size, and (b) oxidative pre-treatment of the carbon black surface.

2. Experimental

2.1 Reagents and equipment

Three commercial Monarch® carbon black samples (M 120, diameter 66 ± 10 nm; M 430, diameter 27 ± 10 nm and M 1100, diameter 14 ± 10 nm) used in this study were obtained from Cabot Corporation (Billerica, MA, USA).

Department of Chemistry, Physical and Theoretical Chemistry Laboratory, University of Oxford, South Parks Road, Oxford OX1 3QZ, UK. E-mail: richard.compton@chem.ox.ac.uk; Fax: +44 (0)1865 275 410; Tel: +44 (0)1865 275 413

4-Nitroaniline, 98%, was purchased from Lancaster Synthesis (Morecambe, UK). 1,4-Dioxane was supplied by Rathburn Chemicals (Walkerburn, Scotland). All other chemicals were purchased from Aldrich (Gillingham, UK). All the reagents were used without further purification. All solutions were prepared using deionised water of resistivity not less than 18.2 MΩ cm^{-1} at 298 ± 2 K (Millipore UHQ, Vivendi, UK).

Electrochemical measurements were recorded using an Autolab PGSTAT 20 computer-controlled potentiostat (EcoChemie, Utrecht, The Netherlands) with a standard three-electrode configuration. A glassy carbon electrode (GC, 3 mm diameter, BAS Technical, UK) was used as the working electrode. A silver–silver chloride (Ag/AgCl) and a carbon rod acted as the reference and counter electrodes respectively. The GC was polished using diamond pastes of decreasing sizes (Kemet, UK). Cyclic voltammetry (CV) was recorded at a scan rate of 50 mV s^{-1} unless stated otherwise. All solutions were thoroughly degassed with pure N_2 for 10 min prior to performing any voltammetric measurements. Electrochemical experiments were carried out at room temperature in pH 7.1 phosphate buffer solution (Na_2HPO_4 and NaH_2PO_4).

Sonication was carried out using a D-78224 Singen/Htw sonicator (50/60 Hz, 80 W, UK). Centrifugation was carried out using a Centrifuge 5702 (Eppendorf, UK). X-Ray photoelectron spectroscopy (XPS) was performed on SAF VG 2 at the Chemical Research Laboratory, Department of Chemistry, University of Oxford, UK, using X-radiation from the Al-Kα band. All XPS experiments were recorded using an analyzer energy of 50 eV for survey scans and 20 eV for detailed scans. The base pressure in the analysis chamber was maintained at not more than 1.0×10^{-6} mbar. Each derivatised carbon sample studied was drop-cast on gold foil and then placed in the ultra-high vacuum analysis chamber of the spectrometer. Analysis of the resulting spectra was performed using XPS Peak 4.1.

2.2 Oxidative pre-treatment of carbon black

In order to increase the number of carboxyl groups on the as-received carbon black surfaces, the as-received carbon blacks were oxidised using the following protocol: the native carbon blacks were sonicated in a mixture of conc. HNO_3 + H_2SO_4 (3 : 1 v/v) for 7 h, except where stated. After which time, the oxidised carbon blacks were centrifuged, extensively washed with deionised water until the washings ran neutral, and then dried under vacuum overnight prior to use.

2.3 Chemical modification of carbon black with 4-nitroaniline

The coupling of 4-nitroaniline to surface carboxylic acid groups on carbon black was achieved as follows: 2 g of carbon black was first stirred in 15 mL of thionyl chloride at room temperature for 90 min to convert the carboxylic acid groups to the corresponding acyl chlorides. Then the mixture was carefully placed in a rotary evaporator in order to remove excess thionyl chloride. The resulting acyl chloride-modified carbon black was then coupled with 4-nitroaniline by stirring the above modified carbon black in 25 mL of 1,4-dioxane to which 4-nitroaniline (0.8 g, 5.79 mmol) and ethyl diisopropylamine (1.7 mL, 10 mmol) were added. After that the reaction mixture was left to stir for 18 h at room temperature. Finally, the modified carbon black was centrifuged, washed with 1,4-dioxane and deionised water to remove any unreacted species and then dried under vacuum.

The removal of physisorbed species on the modified carbon black was studied by soaking 4-nitroaniline modified carbon black in tetrahydrofuran (THF) for 48 h, then centrifuging, washing extensively with THF and then drying under vacuum.

2.4 Modification of glassy carbon electrode with carbon black

The construction of films consisting of modified carbon black on the surface of glassy carbon electrodes was performed as follows: 10 mg of carbon black was suspended in 1 mL of chloroform to form a "casting" suspension. The casting suspension was then briefly sonicated for 2 min in order to disperse the carbon black particles. A 10 μL of this suspension was then pipetted onto the surface of a freshly polished glassy carbon electrode and left to dry in air.

2.5 Boehm titration

The titration procedure for analysis of oxygen-containing functional groups was carried out based on Boehm's[1,2] method together with the recommended methods of CO_2 expulsion, following the procedures of Goertzen *et al.*[25] In general, the Boehm titration proceeded as follows: three portions of a known mass (*ca.* 2 g) of carbon black was added into 10.00 mL of three different reaction bases of 0.05 M concentration: $NaHCO_3$, Na_2CO_3 and NaOH. The samples were agitated by stirring for 24 h and then centrifuged to remove the suspended carbon. Aliquots of 5.00 mL of each sample were taken and excess 0.05 M HCl was added to neutralise the remaining reaction base: 15.00 mL of HCl was added to the $NaHCO_3$ and NaOH aliquots, while the aliquots of Na_2CO_3 were acidified with 20.00 mL of HCl. The acidified solutions were then degassed with N_2 for 2 h to remove dissolved CO_2 from the solutions. After that each sample was then back-titrated with 0.05 M NaOH with continuous degassing during the titration. In terms of the endpoint determination, we used both pH meter and colour indicator. Our observations support those of Goertzen and co-workers[25] that there is no significant difference between titrations conducted using either pH meter and/or colour indicator to detect the end point. The indicator employed was bromothymol blue (BDH, Poole, UK).

As the strongest base, NaOH is assumed to neutralise all Brønsted acids (including phenols, lactones and carboxylic acids), while Na_2CO_3 neutralises carboxylic and lactonic groups and $NaHCO_3$ neutralises carboxylic acids. From this knowledge, the amounts of various oxygen surface functional groups can be determined by using eqn (1):

$$n_{CSF} = \frac{n_{HCl}}{n_B} \cdot [B] \cdot V_B - ([HCl] \cdot V_{HCl} - [NaOH] \cdot V_{NaOH}) \cdot \frac{V_B}{V_a} \quad (1)$$

where n_{CSF} is the moles of carbon surface functionalities that reacted with the reaction base added during the mixing step. [B] and V_B are the concentration and volume of the reaction

base mixed with the carbon black, giving the total number of available moles of reaction base that can react with the surface functionalities on carbon black. V_a is the volume of the aliquots taken from the V_B. [HCl] and V_{HCl} are the concentration and volume of acid added into the aliquots pipetted from the original sample, providing the number of accessible moles of acid added to the aliquots which can react with the remaining reaction base. $\frac{n_{HCl}}{n_B}$ is the molar ratio of acid to base taken into account for monoprotic and diprotic reaction bases. While [NaOH] and V_{NaOH} are the concentration and volume of the titrant in the back-titration, referring to the moles of the titrated base reacting with the remaining acid. Consequently, the exact number of moles of the remaining reaction base can be determined as we know the amount of acid reacted with the remaining reaction base through the titration. The difference of the initial and the remaining amount of reaction base results in the amount of reaction base reacted with the surface functionalities on carbon black. The amount of surface functionalities (n_{CSF}) is then calculated.

3. Results and discussion

3.1 Boehm titration of oxidised and non-oxidised samples

Boehm titration allows the quantification of acidic groups present on the surface of carbon black (CB).[1,2,25] Without their deliberate introduction, acidic groups based upon elements other than carbon and oxygen are typically present in only trace quantities in CB samples. Oxygen functionalities typically dominate, owing to the natural abundance of oxygen during and after CB production.[3,4] Further oxidation can introduce additional oxygen functionalities to the surface of the CB, as well as oxidise existing functionalities to higher oxidation states. In this work, CB was deliberately oxidised, where noted, by sonicating in a mixture of concentrated HNO_3 and H_2SO_4 (3 : 1 v/v).

By quantifying the amount of excess $NaHCO_3$ neutralised by a known mass of CB, the number of carboxylic acid groups on the CB can be determined. The amount of Na_2CO_3 neutralised corresponds to carboxylic acid and lactonic groups. The strongest base, NaOH, is assumed to neutralise all moderately strong Brønsted acids present, *e.g.* phenols, lactones and carboxylic acids. Using this technique the acidic functional groups on the surface of the CB M 430 was quantified before and after being oxidised for 7 h, and the values are shown in Table 1. Oxidation in the acidic solution results in the removal of virtually all lactonic groups, presumably by hydrolysis. The number of phenolic groups is also reduced, presumably due to hydrolysis and oxidation to carboxylic acid groups. The number of carboxylic acid groups increased by approximately a factor of three after oxidation, which is the result of the hydrolysis and oxidation of lactones, phenols, quinone, *etc.* as well as carbon on the edge sites of the quasi-graphitic lattice.[3,4,12,18]

Table 1 Carbon surface functionalities on native and acid-oxidised Monarch® 430 carbon black

Carbon material	Functional groups	Amount of carbon surface functionalities, n_{CSF}/μmol g^{-1}
M 430, as received	Carboxylic	24 ± 2
	Lactonic	7.5 ± 2
	Phenolic	25 ± 4
M 430, oxidised in HNO_3 : H_2SO_4 for 7 h	Carboxylic	79 ± 8
	Lactonic	0.3 ± 0.3
	Phenolic	18 ± 6

3.2 Immobilisation of 4-nitroaniline on the carbon black surface

CB samples were modified by 4-nitroaniline (NA), either by the physisorption of NA onto (or intercalation into) the CB particles surface, or by chemical (covalent) tethering of NA to the CB surface. The full procedures for physisorption and covalent tethering are detailed in the Experimental, and similar processes have been previously reported.[10,13,14] Briefly, physisorption occurred when CB was stirred in 1,4-dioxane containing 200 mM NA. Non-associated NA was removed by extensive washing of the isolated CB with 1,4-dioxane and water. Covalent tethering was achieved by the activation of carboxylic acid groups on the surface of the CB with $SOCl_2$ (Scheme 1) followed by nucleophilic addition to NA to yield CB with nitrobenzene covalently tethered to the surface *via* an amide linkage. X-Ray Diffraction (XRD) did not display any significant differences in the structure of the CB after exposure to NA.

3.3 XPS analysis of the modified carbon

X-Ray Photoelectron Spectroscopy (XPS) analysis was carried out on covalently modified CB M 430 in order to confirm the presence of NA on the CB surface. A wide survey scan was performed over the range of 100–1400 eV for CB before and after covalent tethering of NA, and Fig. 1 displays the X-ray photoelectron spectra of (a) non-oxidised and (b) 7 h oxidised CB after covalent tethering of NA. Three main spectral peaks can be observed in the survey scan with the binding energy of *ca.* 293.8 eV, 409.3 eV, and 541.2 eV corresponding to the emission from C_{1s}, N_{1s} and O_{1s} levels respectively. Other two spectral peaks were observed at *ca.* 982 and 1233 eV corresponding to the O_{KLL} and C_{KLL} Auger emissions, respectively. Detailed analysis with thirty repeat scans over each of these three principal regions was recorded to obtain quantitative data. The percentage elemental composition of each element was determined from the area under each peak, and is shown in Table 2. The results clearly demonstrate that no N is detected for the blank material, but after treatment with $SOCl_2$ and NA, N is present on the CB surface. Oxidation of the surface results in an increase in both O and N, consistent with the oxidation step introducing more ArCOOH groups (as demonstrated by Boehm titration of the samples in Section 3.1) and consequently more NA present on the CB surface. However, it should be noted that XPS is only approximately quantitative, as the roughness and porosity of the CB material results in only the most exposed areas of the CB being recorded. To clarify the quantity of 4-nitroaniline on the whole surface of the carbon black, voltammetric analysis was carried out.

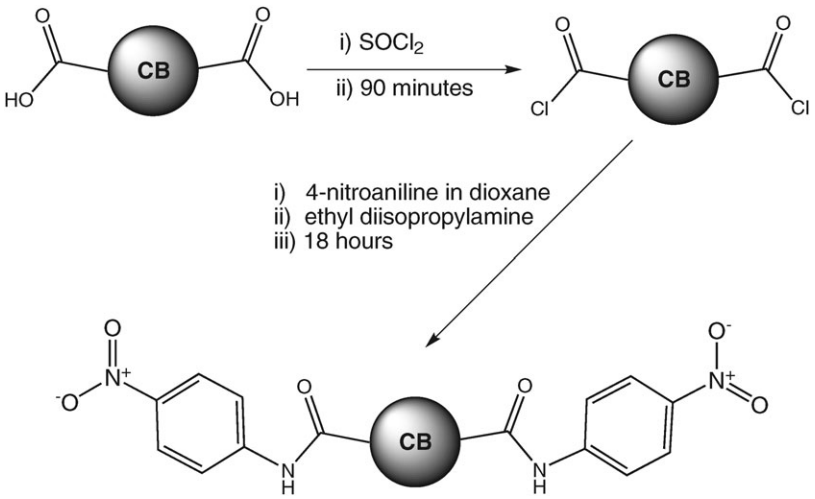

Scheme 1 The modification of CB with NA *via* the conversion of surface carboxyl groups to the corresponding acyl chlorides.

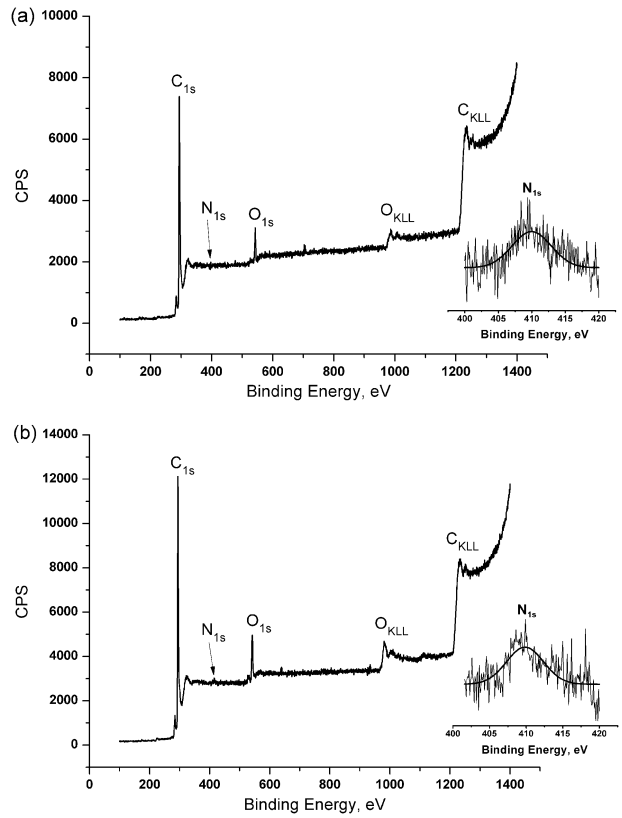

Fig. 1 Wide scan XPS spectra (100–1400 eV) for CB M 430 covalently modified with NA. The samples relate to CB that were either (a) unoxidised or (b) oxidised for 7 h prior to covalent tethering. Inset displays detailed scans in N_{1s} region.

Table 2 The percentage elemental composition of the NA-labelled and native carbon black surfaces using XPS.

Material	%C	%O	%N
Native CB M 430	90.4	9.6	—
NA-labelled-CB M 430	86.8	11.0	2.2
NA-labelled-CB M 430 (oxidised)	84.1	12.9	3.0

3.4 Characteristic voltammetry of NA on the CB surface

Fig. 2 displays a scan at a clean GC electrode recorded in pH 7.1 phosphate buffer, overlaid with a scan for the same electrode in the same solution after *ca.* 0.1 mg of CB was drop-cast on the GC surface. After being modified with the CB there is a clear increase in non-faradaic charge, associated with a significant increase in the active surface area of the electrode, as well as the semi-conducting nature of the drop-cast layer of CB particles.

Fig. 3 displays a scan recorded for CB non-covalently modified with NA (*e.g.* stir in NA solution, isolate CB and wash extensively, as described in Section 3.2) drop-cast on the surface of a GC electrode. Scanning in the potential range *ca.* +0.5 V and −1 V *vs.* Ag/AgCl, only a single large reduction wave (labelled peak **I**) is observed at *ca.* −0.75 V. A shoulder can be observed in the CV at *ca.* −0.9 V; shoulders or multiple peaks were frequently observed in other experiments, and all of the processes observed in this region are hereafter referred to as System I. No other redox processes

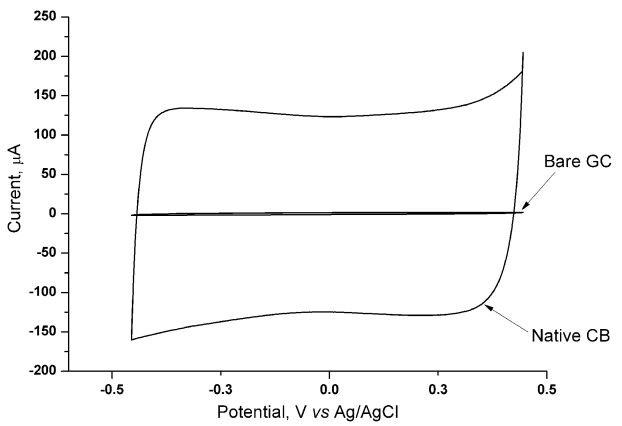

Fig. 2 Overlaid cyclic voltammograms for a bare glassy carbon (GC) electrode (diameter 3 mm), and after drop-casting *ca.* 0.1 mg unmodified (native) CB on the GC electrode. Recorded in degassed pH 7.1 phosphate buffer solution at 50 mV s^{-1}. All other scans are recorded under the same conditions, unless otherwise noted.

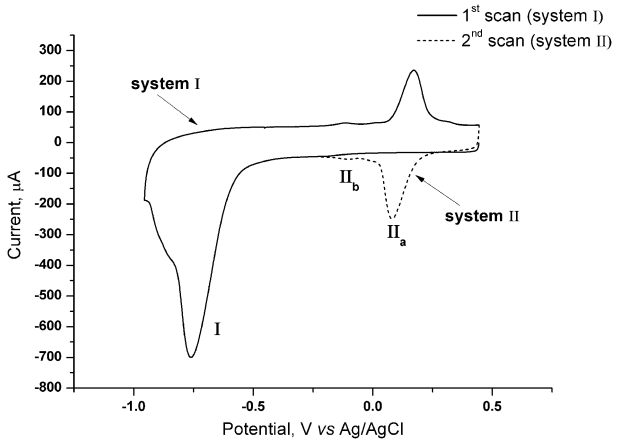

Fig. 3 Cyclic voltammogram of GC drop-cast with carbon black M 430 modified by exposure to NA over the regions of System I (solid line) and System II (dashed line).

were observed prior to this system, and after scanning into System I no faradaic processes were observed in this potential region on the 2nd and subsequent scans. However, after scanning into System I a reversible couple was generated at *ca.* +0.1 V *vs.* Ag/AgCl (denoted System II, labelled $\mathbf{II_a}$). In addition a significantly smaller redox couple was also observed at *ca.* −0.2 V *vs.* Ag/AgCl (labelled $\mathbf{II_b}$).

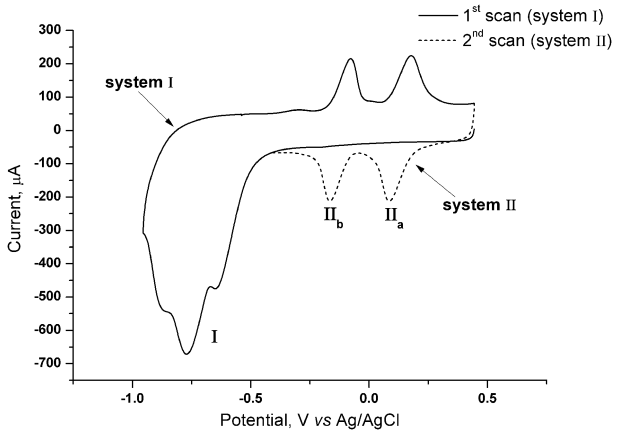

Fig. 4 Cyclic voltammogram of GC drop-cast with carbon black M 430 modified by exposure to $SOCl_2$ followed by covalent tethering of NA over the regions of System I (solid line) and System II (dashed line).

Fig. 4 displays a scan recorded for a GC electrode with covalently-tethered NA-modified CB drop-cast on the surface. Similar behaviour was observed to that noted above for CB non-covalently modified with NA, except the redox couple $\mathbf{II_b}$ was significantly larger following the covalent-tethering process.

The reduction process on the first scan (System I) is well known for surfaces modified with nitroaryl groups,[10–12] and corresponds to the reduction of the nitro group to a mixture of $ArNH_2$ and ArNHOH (Scheme 2). The multiple peaks and shoulders observed correspond to the two different reduction pathways, as well as the different chemical environments expected for surface-bound NA due to the heterogeneous nature of the CB surface. The relative ratio of amine to hydroxylamine products is known to be related to the solvent employed and other experimental conditions.[11,12,26] The two redox processes observed in System II ($\mathbf{II_a}$ and $\mathbf{II_b}$) are attributed to the same electrochemical mechanism occurring in two distinct chemical environments of the CB surface. Based upon extensive previous literature,[10–12,22–24,27] the electrochemical process is the two electron, two proton quasi-reversible ArNHOH/ArNO redox couple (Scheme 2) corresponding to ArNHOH groups electrogenerated in System I.

Repeated cycles were recorded for the non-covalently modified CB sample (Fig. 5). The peaks for $\mathbf{II_a}$ were observed to decrease in height with successive scanning before forming relatively stable peak heights after *ca.* 50 scans, while $\mathbf{II_b}$ did not change significantly with repeated scanning (exceptions discussed in more detail later). After *ca.* 50 scans to stabilise the system, a scan-rate study (Fig. 6) demonstrated that the peak current, I_p, for both $\mathbf{II_a}$ and $\mathbf{II_b}$ was linear with respect to the scan rate (plotted as an inset in Fig. 6) as opposed to the square-root of scan rate typically observed for diffusion-limited processes, therefore demonstrating that both processes correspond to surface bound species.

Given the significant increase in $\mathbf{II_b}$ following reaction of the CB with $SOCl_2$ (*cf.* Fig. 3 and 4) it is inferred that $\mathbf{II_b}$

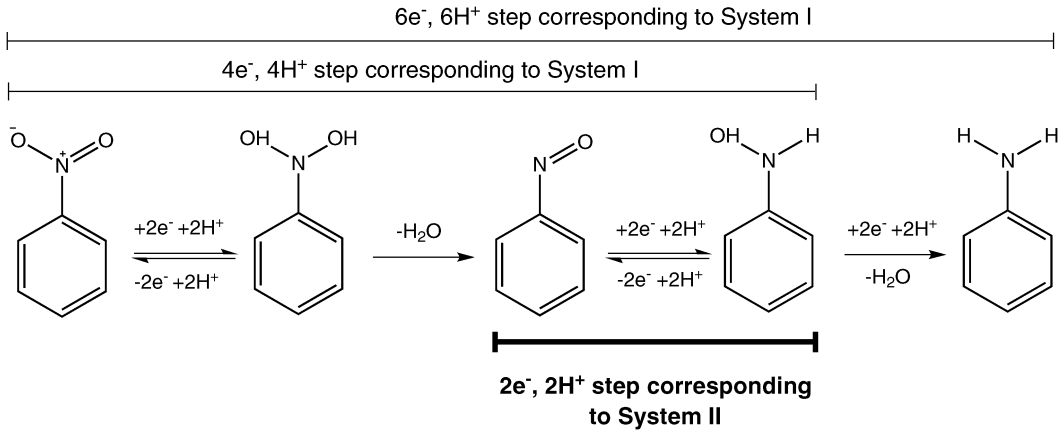

Scheme 2 The general mechanism for the electrochemical reduction of a surface-bound arylnitro group in aqueous media, exemplified here by nitrobenzene.

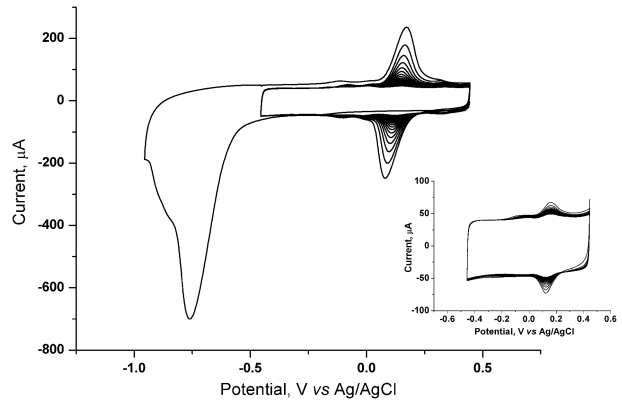

Fig. 5 Twenty consecutive cyclic voltammograms of CB M 430 modified by exposure to NA (without reaction of $SOCl_2$) drop-cast on a GC electrode. Inset: cyclic voltammograms over the region of System II (initial scan into System I not shown) for the same CB after being soaked in THF for 48 h to remove physisorbed molecules.

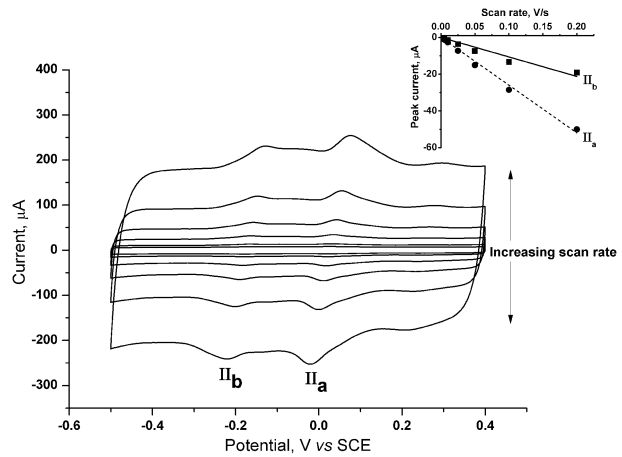

Fig. 6 Overlaid scan rate study (5–200 mV s^{-1}, after *ca.* 50 scans at 50 mV s^{-1} to stabilise the system) in the region of System II for CB M 430 modified by exposure to NA drop-cast on a GC electrode. Inset: plot of peak current *vs.* scan rate for the reduction peaks in $\mathbf{II_a}$ (●, dashed line, $R^2 = 0.995$) and $\mathbf{II_b}$ (■, solid line, $R^2 = 0.997$).

corresponds to the reduction of nitroaryl groups covalently tethered to the CB surface. The small $\mathbf{II_b}$ peaks observed without $SOCl_2$ treatment (Fig. 3) are believed to stem from another reaction to form covalently tethered NA. Lactone groups are commonly present on the surface of the CB,[1,2] and were demonstrated by Boehm titration to be present in the non-oxidised CB samples used in this work (Section 3.1). Sterically strained lactones, as well as acid anhydride species are known to undergo nucleophilic attack by amines.[18]

The redox couple $\mathbf{II_a}$ was present to similar degrees in both $SOCl_2$ and non-$SOCl_2$ treated samples. Therefore this redox couple does not correspond to covalently bound nitroaryl compounds, nor acid–base pairs formed between acidic groups (*e.g.* carboxylic acid) on the CB surface and NA. The large surface area of CB is likely to result in extensive amounts of adsorption at the surface. After exposure of the CB to NA, the CB was washed extensively with water to remove loosely associated material. However, it was found that bathing in a large excess of THF for 48 h resulted in a decrease in the size of $\mathbf{II_a}$ (inset in Fig. 5), implying that some of the material is loosely physisorbed. This also accounts for the initial decrease in the peak size with successive scanning. However, other material was not removed by bathing, washing and cycling, and is therefore strongly associated with the CB surface. It is probable that some of this relates to NA groups strongly physisorbed at favourable sites on the CB surface. Some of the material is also likely to be intercalated. The intercalation of benzylamine has previously been demonstrated at defect sites in carbon nanotubes.[22,24] Given that the CB particles employed in this work have irregular graphitic surfaces and the graphitic planes are of nanoscale dimensions, it is feasible that intercalation (at the numerous defect sites, as well as potentially between the relatively small graphitic layers found at the nanoscale) would occur to some extent. Evidence presented later in this work indeed indicates that significant intercalation occurs, particularly for the smallest particles employed in this work. Alternatively, such behaviour might correspond to other physical processes that closely resemble intercalation, for example insertion into microscale pores, crevices, clefts, and other surface defects. However, since $\mathbf{II_a}$ appears to correspond to both physisorption and intercalation processes, and occur to different degrees for different samples, both processes will be grouped under the general heading of 'physisorbed NA' for convenience. These various mechanisms and quantification of their relative contribution to $\mathbf{II_a}$ are under further investigation.

The *ca.* 0.4 V difference in peak potentials between $\mathbf{II_a}$ and $\mathbf{II_b}$ implies different orientation and interaction between the NA groups and the CB. For the previously reported quantification of carboxylic acid groups on CB with 3,4-dihydroxybenzylamine, the voltammetry of covalently bound (through the amine group) and physically adsorbed molecules were observed at the same potential.[7] The different potentials observed in the case of nitroaniline can be attributed to two factors. Firstly, the planar nitroaniline is expected to 'physisorb' parallel to the basal planes of the CB,[28] while the covalently-tethered species will sit more edge-on, thus altering the kinetics of the reduction process, as well as the electron density of the aryl rings. Secondly, physisorbed NA possesses an amine, a strongly electron-donating group; in covalently-tethered NA this group has been converted to the more weakly donating amide moiety. In the case of 3,4-dihydroxybenzylamine,[7] the probe molecule is less planar and the amine group is not conjugated with the electroactive (dihydroxybenzene) group.

3.5 Ratio of amine and hydroxylamine groups formed

Any quantitative relationships drawn from either the electrochemical reduction of $ArNO_2$ (System I) or the redox couples corresponding to electrogenerated ArNHOH groups (System II) must first address the complexity of System I. For example, System I is a mixed process hence the charge under System I cannot be directly related to the number of moles, while the charge under System II represents a fraction of the original number of $ArNO_2$ groups.

Scheme 2 displays the reduction process for $ArNO_2$, which can correspond to either a 4 e^- process (to ArNHOH), a 6 e^-

process (to $ArNH_2$), or more commonly a combination of the two.[11,12,27] Since the molecules are surface-bound a number of additional 'dimerisation' routes (such as the formation of azo species)[26] can be disregarded. By quantifying the ArNHOH groups (*e.g.* the charge under the System II processes, Q_{II}), the 4 e^- contribution to the reduction process of $ArNO_2$ (System I, with charge Q_I) can be quantified. The remaining charge in System I ($Q_I - Q_{II}$) therefore corresponds to the 6 e^- formation of $ArNH_2$, and knowing this the total number of moles of $ArNO_2$ initially present can be quantified. The total number of modified ArCOOH groups can then also be quantified by investigating the reduction peak of $\mathbf{II_b}$ and applying the observed stoichiometry of ArNHOH groups to $ArNO_2$ groups.

The $Q_I : Q_{II}$ ratio gives the proportion of $ArNO_2$ groups that are reduced to ArNHOH groups. However, it was observed in this work that the $Q_I : Q_{II}$ ratios were not constant, despite keeping experimental conditions (electrolyte, electrode preparation, temperature, scan rate, *etc.*) consistent throughout. This is believed to be due to the fact that System I relates to NA groups over a wide range of possible environments, which resulted in poorly resolved waves with multiple shoulders and peaks. This fact, as well as potentially slow kinetics for some orientations and the non-linear baseline resulting from extensive double layer charging, is believed to have resulted in errors in the integration of the most poorly resolved voltammetry relating to System I. A general value had to be estimated, and by using the values of Q_I and Q_{II} from the detailed analysis of 16 experiments, it was determined that 29 ± 11% of $ArNO_2$ groups were electrochemically reduced to ArNHOH, the remaining 71 ± 11% being reduced to electrochemically-inactive $ArNH_2$.

3.6 Effect of CB oxidation time on the physisorption of NA on CB

The oxidation of CB in the presence of acids and/or oxidising agents is well established to introduce oxides on the carbon surface.[1–4,6,7,25] These oxide groups modify the material properties of the CB,[3,7] as well as providing useful moieties for the introduction of surface modifiers such as nanoparticles and covalently tethered functional groups.[13–17] The effect of surface oxidation on physisorption, either onto (surface physisorption) or into (intercalation) the CB, was investigated by sonicating the CB M 430 in the presence of 3 : 1 $HNO_3 : H_2SO_4$ for 0, 3.5, 7 and 14 h, then bringing the CB into contact with a solution of NA, as outlined in the Experimental section. Afterwards the modified CB was drop-cast onto a GC electrode and scanned through Systems I and II, as described previously. The charge under $\mathbf{II_a}$ was determined for the 2nd scan, and Fig. 7 displays a plot of charge (both as a function of weight and estimated surface area) *vs.* oxidation time. It can clearly be observed that as oxidation time is increased the relative amounts of physisorption decreases. This agrees with previous reports.[28] It has been speculated that oxidation of graphitic layers will reduce the electron-density and thus reduce the amount of physisorbed aryl compounds. While possible, the inductive effect is likely to be weak over large basal planes. Alternatively, donor–acceptor

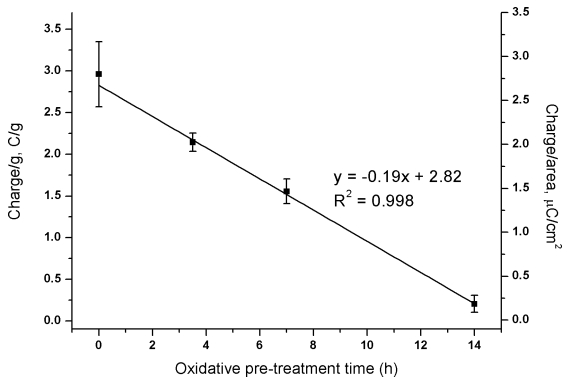

Fig. 7 Plot displaying the effect of oxidative pre-treatment time on the physisorption of NA into CB M 430. Error bars determined by conducting the experiments in triplicate.

complexes featuring carbonyl groups have been postulated as the first sites of physisorption of aryl compounds, followed by physisorption at the basal plane at higher concentrations. Oxidation of the CB removes the carbonyl compounds, thus significantly decreasing physisorption of aryl compounds at low concentrations.[28]

The covalent tethering of redox probes to RCOOH groups has been suggested as a means of quantifying the degree of oxidation of CB surfaces.[7] This work demonstrates that the physisorption of NA is also an excellent means of quantifying the degree of surface oxidation.

3.7 Effect of CB primary particle size on the physisorption of NA on CB

The relationship between the primary particle size of the CB and physisorption of NA was investigated in a similar manner to that used to investigate the effect of oxidation time on physisorption (Section 3.6). The three CB materials investigated (primary particle diameters 14, 27 and 66 nm) were exposed to NA without any prior oxidation, and the quantity of physisorbed material quantified by cyclic voltammetry. Fig. 8 displays the plot of charge (both as a function of weight and estimated surface area) *vs.* primary particle size. The smallest particle size clearly displayed the largest degree of physisorption, both per gram and per cm^2. If taken in terms of

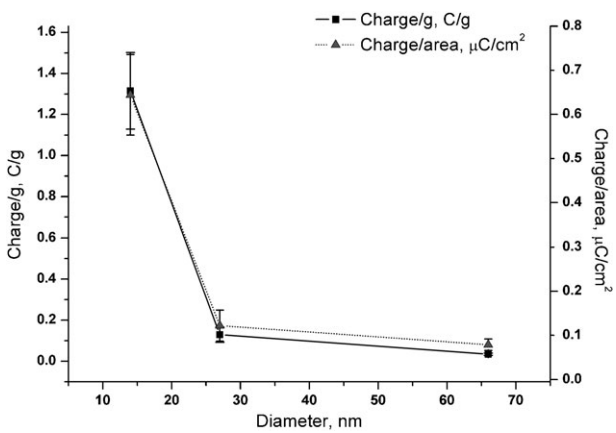

Fig. 8 Plot displaying the relationship between CB primary particle size (diameters 14, 27 and 66 nm) on the physisorption of NA into CB.

simple surface physisorption, the latter observation is somewhat surprising as the smaller particles are not expected to display significantly more planar basal sites (*e.g.* that favour physisorption) per cm^2 than the larger particles. However, the latter observation makes sense if intercalation becomes the dominant form of interaction, with the smaller graphitic planes being more easily displaced and therefore facilitating intercalation. Alternatively, the smaller particles could possess a significantly larger number of quinone groups on their surface, thus enhancing the adsorption of NA.[28]

3.8 Effect of CB primary particle size on the covalent tethering of NA to CB

The three CB materials investigated in Section 3.7 with regards to physisorption (primary particle diameters 14, 27 and 66 nm) were also investigated to determine the effect of primary particle size on the covalent tethering of NA to their surfaces. The CB samples were oxidised with acid for 7 h, treated with $SOCl_2$ (as described in the Experimental and demonstrated by Scheme 1) and their cyclic voltammetry recorded. The physisorption peak ($\mathbf{II_a}$) was relatively small due to the oxidation of the CB surface, although the trend in $\mathbf{II_a}$ *vs.* particle diameter followed that previously described for the samples prepared without $SOCl_2$. The trend in charge under the reduction peak for $\mathbf{II_b}$ *vs.* primary particle size is displayed graphically in Fig. 9. It can be observed that CB with primary particle diameters of 14 and 27 nm possess the highest charge per gram, while particles with diameters of 27 and 66 nm possess the highest charge per cm^2. It is therefore apparent that covalent tethering proceeds to a relatively higher degree on the largest particles, while the smaller particles appear to have much lower surface coverage. The middle particle diameter 27 nm therefore experiences the highest covalent loading of NA in terms of both weight and available surface area.

3.9 Effect of prior handling and oxidation time of CB on the covalent tethering of NA to CB

The influence of any pre-treatment steps of the CB was investigated. Fig. 10(a) displays twenty consecutive CVs recorded for CB M 430 treated with $SOCl_2$ after being taken directly from the sample container, as supplied, and Fig. 10(b) displays twenty consecutive CVs recorded for CB M 430 treated with $SOCl_2$ after oxidising the CB for 7 h. The physisorption peak $\mathbf{II_a}$ decreased with oxidation of the CB surface, as observed previously. The response of the covalently bound redox couple $\mathbf{II_b}$ for the 7 h oxidised sample was observed to be extremely stable, with only minor changes in current throughout twenty consecutive cycles. Bathing the sample in THF for 48 h had no effect upon the size of $\mathbf{II_b}$. However, redox couple $\mathbf{II_b}$ for the 'as received' CB was observed to decrease in height with successive scanning. Similar behaviour has been previously observed for graphite and multiwall carbon nanotubes modified by covalently bonding azo dyes to their surface.[23] In this case electrochemical reduction of the azo group resulted in fragmentation to two amine-functionalised moieties. However, a similar process is not expected to occur here as azo groups are not present, and similar behaviour was not observed for the 7 h oxidised sample. The voltammetric 'fragmentation' or release of NA from the CB surface in Fig. 10(a) therefore relates to the nature of the chemical bond formed between 'as received' CB and NA following exposure to $SOCl_2$.

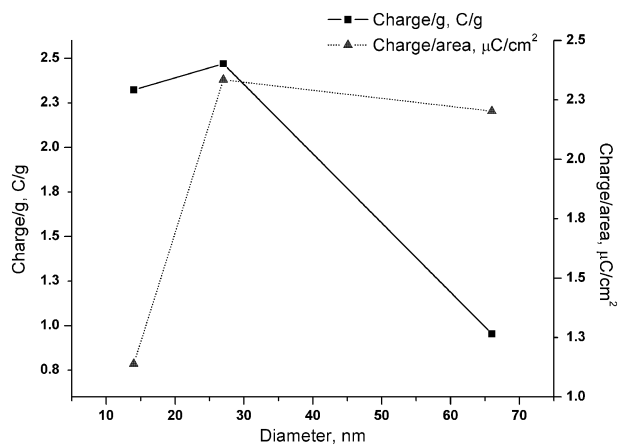

Fig. 9 Plot showing the effect of particle size (primary particle diameter 14, 27 and 66 nm) of CB samples (previously oxidised for 7 h) on the charge relating to the reduction of covalently bound NA ($\mathbf{II_b}$).

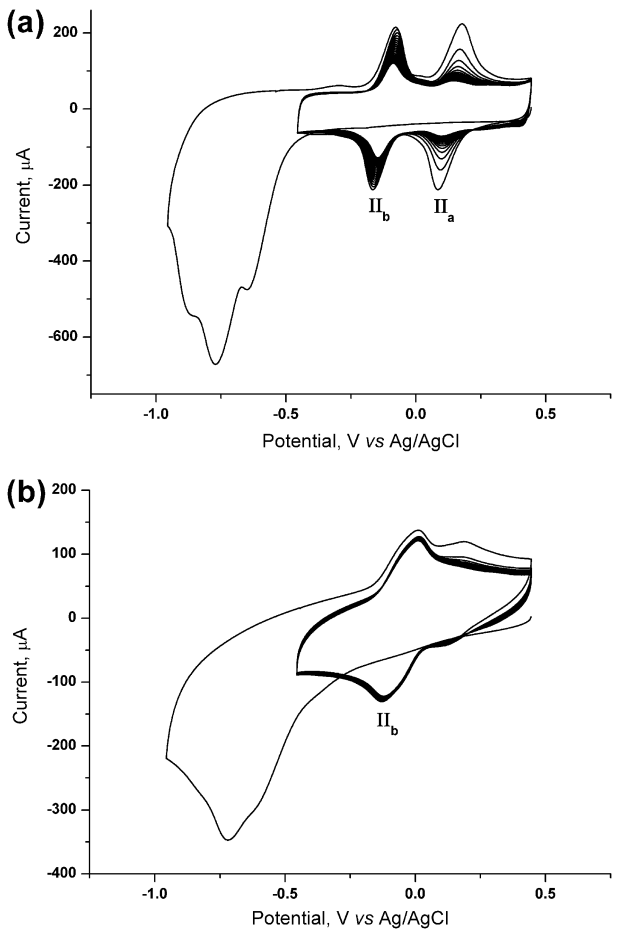

Fig. 10 Twenty consecutive cyclic voltammograms of CB M 430 activated with $SOCl_2$ and reacted with NA, after (a) no prior treatment, and (b) oxidised for 7 h.

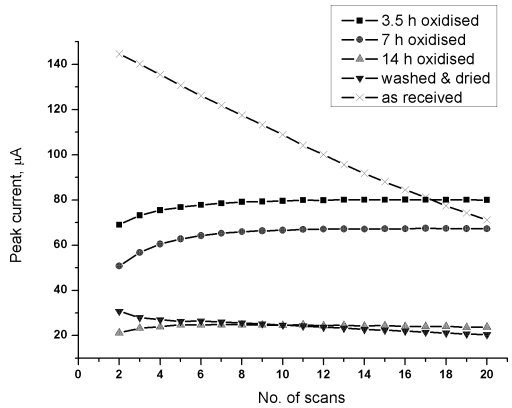

Fig. 11 Detailed plot displaying the trends in peak current with number of scans for the peak corresponding to covalently bound NA ($\mathbf{II_b}$) on CB M 430 as a function of sample pre-treatment: none (CB reacted with $SOCl_2$ as received) (×), sonicated for 7 h in ultrapure water then dried under vacuum (▼), and sonicated in HNO_3 : H_2SO_4 for 3.5 h (■), 7 h (●) and 14 h (▲) to oxidise surface, followed by drying under vacuum.

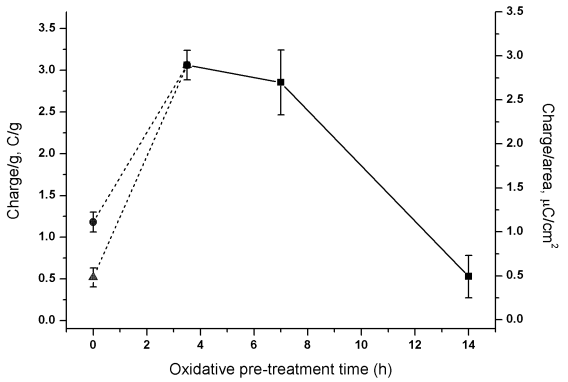

Fig. 12 Plot displaying the effect of oxidative pre-treatment time on the charge corresponding to covalently bound NA ($\mathbf{II_b}$) on CB M 430. For the non-oxidised samples (0 h), the CB was used as received (●), or sonicated for 7 h in ultrapure water then dried under vacuum (▲).

Further experiments were conducted, and Fig. 11 displays the peak current, I_p, for peak $\mathbf{II_b}$ as a function of number of scans. The I_p for the 'as received' sample (denoted by ×) decreased in a linear manner with the number of recorded scans. CB oxidised for 3.5, 7 and 14 h all displayed *ca.* 10% increases in I_p during the first *ca.* 8 scans, before I_p levelled off and remained largely constant. This initial increase in I_p is attributed to changes in the non-faradaic background currents with successive scans; this is partially attributed to significant changes in the size of the nearby peak $\mathbf{II_a}$, although similar trends in I_p were observed regardless of whether the baseline was extrapolated from in front of or behind $\mathbf{II_b}$.

The primary difference in handling between the 'as received' and oxidised CB samples was that the latter were sonicated in aqueous acidic solutions, followed by drying under high vacuum. Two 'as received' samples of M 430 were taken; one was placed under vacuum for 18 h, the other sonicated in ultrapure water for 7 h and then dried under vacuum for 18 h. The results were essentially identical for both forms of handling, indicating that the vacuum step has the most influence on subsequent behaviour (as opposed to aqueous sonication removing surface residues, *etc.*). The I_p for the sonicated, dried under vacuum sample (denoted ▼) is displayed in Fig. 11, and demonstrates a significant reduction in I_p when compared to the 'as received' (×) sample. However, the I_p is also observed to decrease with successive scanning, demonstrating that voltammetric fragmentation is still occurring.

Oxygen is well known to chemisorb dissociatively on graphitic surfaces, forming a variety of oxygen-containing functional groups.[3,4] Thionyl chloride is highly reactive, and is known to react with a wide variety of oxygen-containing functional groups in addition to carboxylic acids, *e.g.* the numerous reactions possible with ketones.[29] It is speculated that for the 'as received' samples, the reactive edge plane sites of the CB have been occupied by dissociatively chemisorbed oxygen, forming a variety of oxygen functional groups. Oxidation of aromatic carbon materials with O_2 has been noted to yield primarily quinones and phenolic groups,[18,26] while HNO_3 in the presence of H_2O yields carboxyl groups.[3,4,30] These O_2-introduced groups react with $SOCl_2$ and subsequently NA, forming relatively weak covalent linkages which are broken with repeated voltammetric scans. Vacuum treatment desorbs the most reactive oxygen functionalities while some remain, resulting in less covalently tethered NA. Any oxidative acid treatment fully oxidises these reactive moieties to more stable species (*e.g.* carboxylic acid groups), resulting in stable amide linkages and completely removing the voltammetric fragmentation that occurs in non-oxidised samples.

It is interesting to note that as the sample oxidation time increases from 3.5 h to 14 h, the I_p for $\mathbf{II_b}$ in Fig. 11 actually decreases. Fig. 12 displays a plot of charge (per g and per cm^2) *vs.* oxidation time. Oxidising the sample for 3.5 or 7 h *ca.* triples the quantity of covalently bound NA, while oxidising the sample for 14 h actually decreases the amount. It should be noted that the trends in Fig. 11 and 12 appear at odds; however, Fig. 11 relates to I_p (*e.g.* qualitative) and Fig. 12 relates to charge (*e.g.* quantitative). Non-oxidised samples lead to narrow sharp $\mathbf{II_b}$ peaks, while oxidation leads to increasingly broad peaks, consistent with an increased number of ArCOOH groups present over a wider variety of sites on the CB surface.

There are two possible explanations for the decrease in $\mathbf{II_b}$ with extended oxidation. The first possibility is that the CB is over-oxidised, with ArCOOH being lost as CO_2.[18,26] The second possibility is that the graphitic layers are over-oxidised and conjugation is detrimentally affected, *e.g.* a large number of (potentially aliphatic) carboxylic acid groups are present, but many tethered NA groups are isolated from conductive graphitic planes and are therefore not electrochemically active.

3.10 Surface coverage of covalently tethered NA

The surface coverage, Γ (mol cm^{-2}), of NA covalently bound to the CB surface can be estimated from the area under the reduction peak of $\mathbf{II_b}$ and then using eqn (2):

$$\Gamma = \frac{Q}{nFA} \qquad (2)$$

Table 3 The surface coverage (Γ/mol cm^{-2}) of electrochemically active NA covalently bound on the surface of three different CB samples, before and after oxidative pre-treatment, determined using the reduction peak for $\mathbf{II_b}$. Before oxidation refers to NA bound to a variety of oxygen functionalities; after oxidation refers to carboxyl groups labelled and quantified by NA. Literature values[10] for nitrophenol covalently bound on bamboo-like (b-MWCNT) and hollow multiwall carbon nanotubes (h-MWCNT) have been included for reference

Carbon material	Γ before oxidation/ mol cm^{-2}	Γ after 7 h oxidation/ mol cm^{-2}
M 1100 (d = 14 nm)	0.8×10^{-11}	1.5×10^{-11}
M 430 (d = 27 nm)	3.3×10^{-11}	5.0×10^{-11}
M 120 (d = 66 nm)	2.4×10^{-11}	3.2×10^{-11}
b-MWCNTs[10]	0.67×10^{-11}	1.3×10^{-11}
h-MWCNTs[10]	0.23×10^{-11}	2.4×10^{-11}

where Q is the charge passed (C), F is Faraday's constant (96 485 C mol^{-1}), A is the surface area of the modified carbon black cast onto the GC electrode (determined from the diameter of each type of carbon black together with the density of carbon black, and knowing the amount of carbon black cast onto the electrode surface (cm^2)), and n is the number of electrons transferred (n = 2). Table 3 details the surface coverage for the three different particle sizes of carbon black, before and after oxidative pre-treatment. The appropriate stoichiometry of ArNHOH to $ArNO_2$ was employed.

CB M 430 (the middle-sized carbon black studied) possessed the highest number of covalently-bound NA groups. In all cases 7 h oxidation increased the number of covalently-tethered NA groups (as well as removing voltammetric fragmentation issues). The value of Γ after acid pre-treatment presumably also relates to the number of electrochemically active carboxylic acid groups present on the CB surface.

Literature values for 4-nitrophenol covalently tethered at surface carboxylic acid groups on hollow and bamboo multiwall carbon nanotubes with $SOCl_2$ have been included in Table 3 for reference.[10] This comparison demonstrates the relatively comparable coverage values obtained by using optimised CB materials.

4. Conclusions

The modification of three carbon black samples with 4-nitroaniline has been thoroughly investigated. Boehm titration, X-ray Diffraction and X-ray Photoelectron Spectroscopy have been used to support extensive voltammetric characterisation of the modified samples. Combining nitroaniline with carbon black results in a voltammetric signal corresponding to intercalation and physisorption processes, and a second peak related to lactonic groups present on the CB surface. Introduction of $SOCl_2$ results in covalent tethering of nitroaniline to a variety of (relatively unstable) oxygen functional groups. Oxidation with HNO_3 and H_2SO_4 for up to 7 h significantly increases the number of covalently-bound species, as well as stabilising the voltammetric signal *via* the introduction of carboxylic acid surface groups. Excessive oxidation eventually results in a decrease in the voltammetric response.

Physisorption decreases with the increase in oxidative pre-treatment time, while intercalation seems to dominate for carbon black materials with primary particle sizes of 14 nm. Size effects are present with regards to covalent tethering of nitroaniline. Smaller primary particles (14 nm) result in poor surface coverage, larger particles (66 nm) have good surface coverage values but poor functionality when taken per gram of carbon black. Primary particle sizes of 27 nm offer the best results in terms of covalently tethered groups per cm^2 and per gram.

Acknowledgements

Syngenta are acknowledged for both support and partial funding of this work. Cabot Corporation and James M Brown Ltd are acknowledged for the generous donation of carbon black used in this work, as well as supplying additional details regarding morphology, *etc*. Dr Robert Jacobs and Dr Michael Hayward are thanked for assistance with XPS and XRD, respectively.

References

1 H. P. Boehm, *Carbon*, 1994, **32**, 759–769.
2 H. P. Boehm, *Carbon*, 2002, **40**, 145–149.
3 *Carbons for Electrochemical Energy Storage and Conversion Systems*, ed. F. Béguin and E. Frackowiak, CRC Press, Boca Raton, 2010.
4 *Carbon Nanomaterials*, ed. Y. Gogotsi, CRC Press, Boca Raton, 2006.
5 A. Curulli, S. N. Cesaro, A. Coppe, C. Silvestri and G. Palleschi, *Microchim. Acta*, 2006, **152**, 225–232.
6 S. Yamazaki, Z. Siroma, T. Ioroi, K. Tanimoto and K. Yasuda, *Carbon*, 2007, **45**, 256–262.
7 S. I. Yamazaki, Z. Siroma, T. Ioroi, K. Yasuda and K. Tartimoto, *J. Electroanal. Chem.*, 2008, **616**, 64–70.
8 K. Kinoshit and J. A. S. Bett, *Carbon*, 1973, **11**, 403–411.
9 K. Kinoshit and J. A. S. Bett, *Carbon*, 1974, **12**, 525–533.
10 A. T. Masheter, L. Xiao, G. G. Wildgoose, A. Crossley, J. H. Jones and R. G. Compton, *J. Mater. Chem.*, 2007, **17**, 3515–3524.
11 P. A. Brooksby and A. J. Downard, *J. Phys. Chem. B*, 2005, **109**, 8791–8798.
12 A. J. Downard, *Electroanalysis*, 2000, **12**, 1085–1096.
13 L. Xiao, G. G. Wildgoose, A. Crossley, R. Knight, J. H. Jones and R. G. Compton, *Chem.–Asian J.*, 2006, **1**, 614–622.
14 G. G. Wildgoose, H. C. Leventis, A. O. Simm, J. H. Jones and R. G. Compton, *Chem. Commun.*, 2005, 3694–3696.
15 J. J. Ye, P. Abiman, A. Crossley, J. H. Jones, G. G. Wildgoose and R. G. Compton, *Langmuir*, 2010, **26**, 1776–1785.
16 K. Amine, M. Mizuhata, K. Oguro and H. Takenaka, *J. Chem. Soc., Faraday Trans.*, 1995, **91**, 4451–4458.
17 J. Panchompoo, L. Aldous, L. Xiao and R. G. Compton, *Electroanalysis*, 2010, **22**, 912–917.
18 *Organic Chemistry*, ed. J. Clayden, N. Greeves, S. Warren and P. Wothers, Oxford University Press, Oxford, 2001.
19 A. I. Medalia and F. A. Heckman, *Carbon*, 1969, **7**, 567–582.
20 A. T. Chidembo, K. I. Ozoemena, B. O. Agboola, V. Gupta, G. G. Wildgoose and R. G. Compton, *Energy Environ. Sci.*, 2010, **3**, 228–236.
21 H. C. Leventis, G. G. Wildgoose, I. G. Davies, L. Jiang, T. G. J. Jones and R. G. Compton, *ChemPhysChem*, 2005, **6**, 590–595.
22 G. G. Wildgoose, M. E. Hyde, N. S. Lawrence, H. C. Leventis, L. Jiang, T. G. J. Jones and R. G. Compton, *Langmuir*, 2005, **21**, 4584–4591.
23 G. G. Wildgoose, N. S. Lawrence, H. C. Leventis, L. Jiang, T. G. J. Jones and R. G. Compton, *J. Mater. Chem.*, 2005, **15**, 953–959.

24 G. G. Wildgoose, S. J. Wilkins, G. R. Williams, R. R. France, D. L. Carnahan, L. Jiang, T. G. J. Jones and R. G. Compton, *ChemPhysChem*, 2005, **6**, 352–362.
25 S. L. Goertzen, K. D. Theriault, A. M. Oickle, A. C. Tarasuk and H. A. Andreas, *Carbon*, 2010, **48**, 1252–1261.
26 *Organic Electrochemistry*, ed. H. Lund and O. Hammerich, Marcel Dekker, New York, 2001.
27 S. S. C. Yu, E. S. Q. Tan, R. T. Jane and A. J. Downard, *Langmuir*, 2007, **23**, 11074–11082.
28 J. S. Mattson, H. B. Mark, M. D. Malbin, W. J. Weber and J. C. Crittend, *J. Colloid Interface Sci.*, 1969, **31**, 116–130.
29 J. S. Pizey and K. Symeonides, *Phosphorus Sulfur*, 1980, **8**, 1–8.
30 P. E. Fanning and M. A. Vannice, *Carbon*, 1993, **31**, 721–730.